

**DYNAMICS OF THE GULF OF  
CALIFORNIA (GC). A CASE  
STUDY ON THE INTERNAL  
WAVES USING SYNTHETIC  
APERTURE RADAR (SAR)**

**Pol Carbó Mestre  
Curso 2013/2014**

**Bernardo Shirasago Germán  
María de los Ángeles Marrero  
Díaz**

Trabajo Fin de Título para la obtención  
del título Grado en Ciencias del Mar

DYNAMICS OF THE GULF OF CALIFORNIA (GC). A CASE STUDY ON THE  
INTERNAL WAVES USING SYNTHETIC APERTURE RADAR (SAR)

*Datos personales del estudiante:*

**Pol Carbó Mestre**

Grado en ciencias del Mar

Curso 2013/14

Universidad de las Palmas de Gran Canaria, Facultad de Ciencias del Mar.

Bajo el programa de movilidad EEUU-América Latina, en la Universidad Autónoma de Baja California Sur y el Instituto Politécnico Nacional, Centro Interdisciplinario de Ciencias Marinas.

pol.carbo101@alu.ulpgc.es

*Datos personales del tutor y cotutor:*

**María de los Ángeles Marrero Díaz**

Universidad de las Palmas de Gran  
Canaria

Facultad de Ciencias del Mar

Departamento de Física

**Bernardo Shirasago Germán**

Instituto Politécnico Nacional, Centro  
Interdisciplinario de Ciencias Marinas

Departamento de Oceanología.

Laboratorios oceanografía Física

## Abstract

In this paper the internal waves generated in the northern part of the Large Islands which propagate northward Gulf of California (GC) have been described using Synthetic Aperture Radar (SAR) images, to expand the knowledge that we have of this waves briefly studied in the GC with such satellite tools. Six SAR images provided by the European Space Agency (ESA) from the ERS 2 and Envisat satellites, taken between May and September 2006, were used. The great potential of using SAR images in the study of internal waves has been proved. A much more complex dynamics than the ones described by other authors has been observed. Three main wave groups are detected according to their propagation, orientation and location. Furthermore, for the first time it has been possible to relate generation moments of one group of waves with a particular tide phase in the northern mouth of the Ballenas Channel. Also, the Peninsula side, north to the Large Islands, has been established as a zone of internal waves generation. Shoaling effects and interference between waves have been qualitatively described.

## Table of Contents

1. Introduction	1
2. Dynamics of the Gulf of California	2
2.1. Meso and macroscale phenomena and the Gulf of California	2
2.2. Internal Waves in the Gulf of California	4
3. Principles of Synthetic Aperture Radar and Internal Waves	6
3.1. Synthetic Aperture Radar Operation	6
3.2. Internal Waves Theory	8
3.3. Radar imaging of Internal Waves	10
4. Study case. Internal waves in the Northern Gulf of California.	11
4.1. Material and methods	11
4.2. Study area	12
5. Results	14
6. Discussion	19
7. Conclusions	21
8. Acknowledgments	22
9. Bibliography	22

## List of figures

- Figure 1: Bathymetry of the Gulf of California (depth in meters), its divisions and names of the basins and points of interest. Modified from Marinone and Lavin (2003). 14
- Figure 2: The Six SAR images used in the present study. Land areas in white. 15
- Figure 3: Fronts of the wave trains with North propagation direction. Each color corresponds to the image in which the wave appears. The dashed lines (for image 731) indicate that the SAR image didn't cover all wave, and these extends beyond the left side. ESRI ArcMap 9.3. 17
- Figure 4: Fronts of the wave trains with East propagation direction. Each color corresponds to the image in which the wave appears. The dashed lines (for image 522 and 715) indicate particular features of that waves, described and discussed in the corresponding section. ESRI ArcMap 9.3. 18
- Figure 5: Fronts of the wave trains just north of the Ángel de la Guardia Island. Each color corresponds to the image in which the wave appears. ESRI ArcMap 9.3. 19
- Figure 6. Tide diagrams of corresponding images days 629, 715 and 731. 19  
Time when the images were taken (red). Vertical axis in cm; horizontal axis in hours. Modified from MAR V0.9, CICESE.

## List of tables

- Table I: Information about SAR image used in the present study. 12

## 1. Introduction

The Gulf of California (GC) is a unique region in the eastern Pacific Ocean for its high biological productivity and diversity, which are due to oceanographic and meteorological processes that occur in it, in addition to their bathymetric features and surrounding orography (Badan-Dagon *et al.*, 1985). Among the oceanographic processes, upwelling and eddies that influence the temperature and biological productivity of the water throughout the whole year should be highlighted. The annual cycle of this semi-enclosed sea is represented by two main seasons, a cold season with strong winds from the northwest (NW) and a warm one with weak winds from the southeast (SE). Besides, the length of the gulf and the differences in their distinct zones also determine the variability of this phenomena (Lavín and Marinone, 2003).

The close contact with the Pacific Ocean involves an influence on this gulf. That influence is represented by the intrusion of the ocean waters into the gulf (Godínez, 2011), by waves of different scales (Obeso-Nieblas, *et al.* 2008; Marinone, 2003) and by its tidal dynamics (Filloux, 1973). This tidal dynamics have of great importance in the area of the Large Islands, the study area of this project, where the intensity of the tidal currents maintains adjacent waters mixed allowing nutrients upwelling and maintaining an important biological productivity throughout the year. These conditions promote the formation of internal waves (Paden *et al.*, 1991) whose effects on the productivity of the area are also important (Gaxiola-Castro *et al.*, 2002). Its description is the main aim of this work.

Internal waves have been observed in all oceans and seas. They originate from the tidal interaction with the local bathymetry. These waves are highly generated during the summer where they travel through a strong and shallow thermocline. Due to the shallow depth of the thermocline and the large amplitude of the internal waves, these can be observed as a rough and smooth bands on the sea surface, mainly due to their interactions with the capillary waves and, in a shorter extent, to biologic and anthropogenic surface films (Alpers, 1985). By the surface reflection, using active sensors, these waves can be detected through satellite tools. By Synthetic Aperture Radar (SAR), a synoptic image of its distribution in a given marine area can be obtained, in which the rough and smooth bands are represented in black and white respectively (Alpers, 1985).

The applicability of these images for the detection of such waves has been demonstrated in numerous studies in different oceanographic regions, such as the Strait of Gibraltar (Brandt, P. *et al.*, 1996); in Massachusetts Bay (Trask and Briscoe, 1983); in the Andaman Sea (Alpers, 1997); in the Sulu Sea (Hsu and Liu, 2004); in the China Sea (Liu., 1998); in the Bay of Bengala (Prasad and Rajasekhar, 2006); and in many other places of the world oceans. SEASAT was the first civilian satellite equipped with a SAR. Currently there are 3 satellites operating: ERS-2, RADARSAT-1 and ENVISAT. Images from ERS-2 and ENVISAT provided by the European Space Agency (ESA) have been used to do the present study.

The aim of this study is the qualitative description of internal waves generated in the Large Islands and propagating in the Northern Gulf of California. Following the work of Fu and Holt (1984), we pretend to expand the knowledge we have about this waves, briefly studied in the Gulf of California with such satellite tools, and set a precedent for future studies. In the present study we expose, from the qualitative analysis of SAR images, some evidence of the distribution of the waves, their forming source, propagation characteristics and their propagation directions. In order to do this, it is necessary to introduce the physical characteristics of the dynamics in the Gulf, its distribution and causes. Also it is necessary to introduce the internal wave theory and the remote sensing principles to detect them.

## 2. Dynamics of the Gulf of California

### 2.1. Meso and macroscale phenomena and the Gulf of California

The Gulf of California (GC) is considered a semi-closed basin to be completely surrounded by a high topography and be connected to the Pacific Ocean in the south (Badan-Dagon *et al.*, 1991). This configuration, combined with the characteristics associated with the tropical-subtropical transition, is determinant in the atmospheric and oceanographic conformation of this environment, where strong seasonal and interannual variations of the physical and biological processes are defined. The wind forcing, tides, the solar impact and the interactions with the Pacific Ocean provide a significant circulation in the Gulf (Badan-Dagon *et al.*, 1985; Lavín and Marinone, 2003; Marinone, 2003).

The atmospheric forcing, as already mentioned, is characterized by weak SE winds in summer and NW winds in winter (Roden, 1964). This wind orientation along the Gulf axis is due to the effect of the adjacent topography (Merrifield and Winnant, 1989). That is why the annual dynamics of the Gulf can be divided into two seasons: warm period and cold period.

Winds parallel to the coastline promote coastal upwelling throughout the year. However, it is on the mainland side during the cold period, with strong NW winds present, where a nutrient-rich water pumping more persistent and effective to the surface occurs (Lavín *et al.*, 1997; Paden *et al.*, 1991). During the warm period, the upwelling on the side of the peninsula is less effective or even zero, because the SE winds are weaker and there are calms frequently, in addition to a narrower shelf and to the existence of an opposite circulation between the surface current and the winds (Lluch-Cota, 2000).

That seasonally and the differences among the upwelling effects of the two periods are clearly reflected in pigment concentrations measured both *in situ* and with satellite tools. With these measures, a highest productivity between November and April coinciding with the upwelling of cold period has been observed. From May, these values fell, with minima in July and August. Then, in November, the winter conditions are restored (Lluch-Cota, 2000).

Other mesoscale phenomenon are eddies. These play an important role, redistributing the nutrient-rich waters from the upwelling zones all over the Gulf. With diameters between 70 and 100 km, the behavior of these eddies determine the distribution of productive waters (Marinone, 2003; Pegau *et al.*, 2002). Generally, anticyclonic eddies (convergent) are associated with high levels of chlorophyll while in cyclonic (divergent) these levels are low. That is the reason because in the first ones the circulation accumulates water in the center, while the second ones to the edges, carrying productive waters to the opposite coast where the upwelling is. Such eddies are distributed throughout the year along the entire Gulf (Marinone, 2003; Pegau *et al.*, 2002). Studies have found that their generation during the warm period is due to the interaction of the Mexican Coastal Current (MCC) with the irregular bathymetry of the area (Zamudio *et al.*, 2008). By the other hand, eddies of the cold period have been less studied and their generation seems to be by wind (Marinone, 2003).



Another important phenomenon in the Gulf of California is the MCC intrusion during the warm season, consisting of oligotrophic waters from the Pacific Ocean along the continental side (Álvarez-Borrego and Schwartzloze, 1979; Lavín and Marinone, 2003; Marinone, 2003; Zamudio *et al.*, 2008). This water is characterized by a lower salinity than the gulf water (Zamudio *et al.*, 2008) and its presence is detected until the northern gulf, being responsible of the generation of a cyclonic gyre there. The intrusion of the MCC is due to a cyclonic circulation in the Pacific, just in front of Cabo Corrientes (Godínez, 2011).

Other large scale oscillations like ENSO (El Niño Southern Oscillation) and PDO (Pacific Decadal Oscillation), also influence on the dynamics of the GC.

Regarding the area of the Large Islands (Ángel de la Guarda, Tiburon, San Lorenzo and San Esteban) due to bathymetric features of the region, tidal currents cause significant mixing, upwelling subsurface cold waters, resulting in a high productivity along the whole year (Pegau *et al.*, 2002; Marinone, 2003). The strong tidal mixing areas are the most biologically productive in the CG (Álvarez-Borrego and Lara-Lara, 1991).

Tides in the Gulf of California (GC) are forced at its entrance by the Pacific Ocean tides, and the length of the gulf makes it almost resonant to the semidiurnal tidal harmonics (Filloux, 1973). This causes large tidal ranges and strong tidal current (up to  $1 \text{ m s}^{-1}$ ) in the shallow area at the northern extreme. The presence of sills among the Large Islands in mid-gulf causes even stronger currents there (up to  $1.5 \text{ m s}^{-1}$ ). The strong tidal currents release large amounts of turbulent kinetic energy, which has a tremendous impact on the physics and biology of the GC. Most of that energy dissipated in the GC is due to the semidiurnal tides, especially  $M_2$  component (García-Silva and Marinone, 2000). In the zone of the sills between the islands, vertical mixing caused by the tidal energy produces strong upwelling of cold nutrient-rich subsurface water (Filonov and Lavín, 2003). The tidal currents are strongly influenced by water stratification (Marinone, 2003), by this is in summer when the highest current intensity forced by tide can be seen.

These conditions described for the Large Islands are linked to the generation of internal waves.

## 2.2. Internal Waves in the Gulf of California

The existence of sills and the presence of high tidal energy, together with a strong stratification that characterizes the Gulf along the whole year, make the appropriate conditions for the generation of internal tides. When the tide passes over a sill, the tidal current accelerates, and internal hydraulic processes distort the thermocline (Paden *et al.*, 1991), radiating a portion of the tidal energy as internal waves. In the GC, the presence of semidiurnal, diurnal and fortnightly components of the internal tide, apparently spreading northward of San Esteban's sill have been found (Filonov and Lavín, 2003), being the semidiurnal the most energetic. Similar results for the Northern GC have been obtained (Jiménez-Lagunes, 2003).

The first evidence of this phenomenon in the GC water column was described by Paden *et al* (1991), at the San Esteban sill. At the same time Badan-Dangon *et al* (1991) recorded the motion of these wave packages with CTD profiles. Evidence of such internal tides as responsible for the distortion of the thermocline was later confirmed by current meter records (Turrent-Thomson, 1996; Ramírez-Manguilar, 2000). The field of internal waves in this area is generated by the barotropic tidal flow over a sill, and is modulated by the cycle of spring and neap tides, with higher activity during spring tides, propagating towards the NW. Part of the energy of the internal tide (10% according to Gaxiola-Castro *et al.*, 2002) becomes solitons packages with wavelength of 1-2 km, traveling in the same direction as the internal tide but along the thermocline (Fu and Holt, 1984; Filonov and Lavín, 2003). The spread velocity of these waves is 1.2 m/s (Fu and Holt, 1984).

Internal waves have important effects on the biology of GC, mixing subsurface water, which contributes to higher levels of nutrients and phytoplankton transport in the water column (Gaxiola-Castro *et al.*, 2002).

The dissipation of the waves produces vertical advection, which results in changes in the distribution of nutrients and temperature. However, they do not produce an effective mixing of the water column, that is, there is no total mixture. Temperature variations are significantly important in subsurface waters, with higher changes in the thermocline, but these variations, besides other parameters such as nutrients, dissolved oxygen, pH and TCO<sub>2</sub> are practically not appreciated at the surface. However, there is a significant increase in chlorophyll both at subsurface and surface waters. This increase is due not only to vertical transport of phytoplankton but also due to the increase in the

concentration of nutrients. The increase in chlorophyll is not immediate, it happens between twelve hours and several days after the wave passes, because phytoplankton acclimation to new conditions of depth and nutrient availability (Gaxiola-Castro *et al.*, 2002).

Previously, Fu and Holt (1984) were the first to describe these internal waves in SAR images in the GC, with which they established that the activity of the internal waves is concentrated mainly in the northern Gulf, north of 28° N, where tides are stronger. They showed the formation of groups of internal waves of short period with a semidiurnal frequency in the northern mouth of the Ballenas Channel and in the channel between two small islands southeast of Isla Tiburón, especially during spring tides, propagating towards the NW along the axis of the Tiburón basin.

The study of these waves in the GC has focused exclusively on the sills and basins associated with the Islands of San Lorenzo, San Esteban and Tiburón and with Ballenas Channel. The objective of this paper is to describe, for the first time using SAR images, the wide distribution and the different spread directions of the internal waves packages generated in the north of the Larges Islands, which propagate around the Northern Gulf of California.

### 3. Principles of Synthetic Aperture Radar and Internal Waves

#### 3.1. Synthetic Aperture Radar Operation

The RADAR (Radio Detection and Ranging) is an instrument capable to detect a target, measure the distance where it is (range) and determinate its position. The term RADAR is commonly used in all active systems using microwave. These equipment are called active because have their own source of energy in target detection, using electromagnetic waves in the microwave range. These waves keep their shape and almost all the transmission power when travel through the atmosphere, other types of gases and even through rain (Shirasago, 1996).

RADAR normal configuration is formed by a transmitter, a modulator and a receiver, operating with an antenna which in most cases are used both for emission and reception. The energy is transmitted by pulses. Part of the pulse is absorbed by the target and another reflected from it. Regarding the latter, one part is lost and the other returns to the emitting source (backscattered signal). The magnitude of the return signal

is measured by the receiver. With the different magnitudes is possible to create different gray levels in an image. Likewise, the travel time of the reflected wave is measured to determine the distance between the receiver and the target.

The radars used in earth's surface imaging can be divided into two categories: The Real Aperture, associated with SLAR acronym (Side Looking Aperture Radar) and Synthetic Aperture or SAR (Synthetic Aperture Radar). The latter is the fundamental tool of the present study.

The Aperture concept is directly related to the radar antenna. The resolution of a radar image is determined by the size of the antenna. With a larger antenna the resolution will be higher. Due to the physical limitations of the antenna's design, the aperture for high-resolution measurements is synthesized. The antenna aperture is defined as the effective area of reception or transmission of an electromagnetic wave, which depends directly on the size of the antenna and the aperture efficiency (Steinberg, 1976). Hence, the synthetic aperture term is related to synthesis or shortening of a large antenna (even kilometers), to a real of smaller size (meters). This is achieved by taking advantage of the position change of the radar during its navigation and the time in which the target is within the radar beam (integration period). During the time of beam illumination on the object, the satellite will have moved a certain distance. Therefore, the retroreflectance caused by the object will be influenced by the Doppler Effect. Accordingly, the resolution depends on the analysis of not only the arrival time of the pulse, but also on their frequency. By an appropriate processing of the received pulses can be synthesize a large antenna by another of few meters.

Another factor to consider in SAR measurements, is the sampled surface, which plays a key role in the signal retroreflected. In the case of smooth surfaces, the radar pulse is reflected specularly, losing the signal and consequently dark areas are formed in the SAR image (areas without information). As the sampled surface roughness increases, the specular reflection decreases, which increases the retroreflectance. That is, for rougher surfaces, the retroreflectance detected by the radar will be greater and therefore the image brightness will increase.

As for the sea surface, the presence of capillary waves and short gravity waves makes it a rough surface detectable by radar. So it is possible to create an image of sea surface to watch the behavior of such waves. Among other phenomena, these short

waves are generated by the wind, so that by measuring the surface roughness can be known the wind intensity and even the direction. As already discussed, other phenomena such as atmospheric waves, sea fronts and internal waves also affect the capillary waves.

The retroreflectance produced by a marine surface with a specific waves pattern, is originated from a resonant phenomenon called Bragg resonance. This is the sum of the phase of the retroreflected signals which generates a strong return signal, so that even emitting low energy pulses, it can continue receiving a return signal strong enough to be detected.

### 3.2. Internal Waves Theory

Internal waves are waves that travel within the interior of a fluid. It owes its existence to the stratified density structure of the two fluids, with a very sharp density change occurring along the interface and with the properties that smaller the density contrast, the lower the wave frequency, and the slower the propagation speed (Alpers, 1985).

Internal waves and solitons, like observed in the GC formed from the internal tide energy, are a class of nonsinusoidal, nonlinear and more-or-less isolated waves of complex shape. The signatures of this waves are made visible by wave/current interaction, which permit make *in situ* observations using almost any ocean instrumentation capable of recording current, density, displacement of plankton layers or similar quantities, and by remote sensing systems.

The formation processes of internal waves vary according to the environment in which they occur. The oceanic internal waves are ubiquitous wherever strong tides and stratification occurs in the neighborhood of irregular topography. They can propagate over several hundred kilometers and transport both mass and momentum, which implies a significant shear velocity and may involve episodes of turbulence and mixing. The mixture usually produces an input of bottom nutrients into the water column and surface, fertilizing local regions where waves are present and influencing the productivity of these areas (Gaxiola-Castro *et al.*, 2002). Due to these characteristics, the generation of internal waves occurs mainly during the warm season, approximately every twelve hours, associated to the semidiurnal tides and more frequently during spring tides. During the neap tides their presence is weak or even zero. The annual

variations of density and the large scale currents also play an important role in their generation.

The nonsinusoidal oscillations predominantly produce downward displacements. The amplitudes are rank-ordered, with largest at the front of the packet and smaller at its rear. The same happens with wavelengths and the crest, with the longest waves at the front of the group. The number of individual oscillations within the packet increases as its age increases, with one new oscillation added per Brunt-Väisälä period. The maximum amplitude of the leading oscillations appears to be related to the magnitude of the downward displacement of the pycnocline during the ebb (offshore) tidal phase.

Exist two types of solitons according to the place where they are generated. The generation phase can occur at the edge of the continental shelf or in sills. During the phase of the barotropic tide, when the flow is outward the platform or the sill, occurs a depression of the pycnocline developed in the deep side of the bathymetry. This suggests that the operative process is the formation of a Lee Wave down-current of a sharp change in the bathymetry (Maxworthy, 1979). Thus, the generation process occurs very close to the edge of the platform. For sills, their generation also occurs more or less in the same geographical point. When the tide passes over the sills the tidal currents accelerate, and internal hydraulic processes distort the thermocline (Paden *et al.*, 1991) radiating part of the tidal energy as internal waves. As already mentioned, this generation varies significantly in terms of bottom slope and water density stratification. Depending of these, the energy of internal tide will propagate offshore or towards the continental shelf (Graig, 1987). An alternative mechanism to Lee Waves generation is direct production of rank-ordered solitons by shear-flow instability just up-current of the edge of shelf or sill. For this case, near the maximum of tidal current, the velocity shear is great enough to excite solitons directly. Because of nonlinearity, their propagation speed can exceed the instantaneous fluid speed, and they move against the current even during maximum flow. With reversal of the tide, they accelerate and move with speed that is the order of the summed phase and current velocities (Haury *et al.*, 1979).

The distance between the packets is the wavelength of the internal tide and the velocity implied by that distance and the tidal period is the nonlinear velocity of the leading soliton (Alpers *et al.*, 1997).

It is in dissipation phase that the shelf- and sill-generated solitons differ the most. In the space beyond a sill, the soliton packets radiate and spread out, adding one new oscillation per buoyancy cycle and moving more or less free of bottom effects, permitting higher lifetimes in open sea. On the shelf, however, the waves suffer increasingly strong bottom interactions as the water shoals.

In their displacement towards the coast, because of their large amplitudes, internal waves quickly turn into nonlinear, becoming unstable and sometimes disintegrating into groups of shorter waves with large amplitudes, which finally dissipate their energy on the coast. Refraction, due to both the shoaling depths and the decreasing pycnocline depth strongly, orients the packet crests along isobaths, retards their speed of advance, and erodes their amplitudes (Sandström and Elliott, 1984). Scattering from depth inhomogeneities contributes to additional attenuation.

### 3.3. Radar imaging of Internal Waves

Due to the existence of a sharp thermocline and their wave amplitudes, is relatively easy to detect internal waves using SAR images. These images are characterized by dark and bright bands representing smooth and rough areas alternately of the sea surface. These bands are caused by the retroreflectance which produces the internal wave modulation on capillary waves (gravity waves of short period) (Shirasago, 1996). The radar sense the short-scale roughness of the ocean surface by means of Bragg scattering. Thus, the radar signatures be the result of a modulation of the short surface waves, generated by interaction with the internal waves; This modulation can either be achieved by surface films (slicks) that accumulate in flow convergence zones and damp short surface waves there, or by hydrodynamic interaction of these waves with the horizontal surface current associated with the internal wave motion (Alpers, 1985).

The first mechanism is often active in coastal waters where surface films, either of natural or anthropogenic origin, are present. These films, even when monomolecular, damp short surface waves very strongly, reducing the radar retroreflectivity accordingly. When slicks modulate the short-scale surface roughness, the radar image of an internal wave field consists of dark streaks (areas of reduced radar backscatter) on a uniform bright background. In most cases, however, the radar signatures of internal waves have a double sign, which means that the corresponding radar image consist of bright and

dark streaks associated respectively with enhanced and reduced radar reflectivity as compared with the local mean, indicative of hydrodynamic modulation (Alpers, 1985).

Moreover, there are currents associated with internal wave. The internal waves cause almost no elevation of the surface and are associated with a spatially and temporally varying surface current field which interacts with the surface waves, giving rise to the surface-roughness modulation. These surface currents generate convergent zones where capillary waves are concentrated generating a high roughness surface band and consequently a bright band in SAR image. By contrast, in areas where surface streamlines are divergent, capillary waves disintegrate forming smooth surface and consequently dark bands in the SAR image. With this waves, the associated radar image therefore consists of pair of adjacent bright and dark bands on a uniform background. The leading edge of the nonlinear internal wave train is associated with a convergence zone, giving rise to a bright band in the radar image (Alpers, 1985).

The mentioned above, explain the principles which permit seeing internal waves in SAR images. According to Robinson (1987), their representation in SAR images as a function of intrinsic features of the waves and the visualization characteristics associated with radar signatures, present the following traits:

- The waves are detected in packets of 4 to 20.
- The crests are normally parallel to the bathymetry.
- The waves appear dark on a bright background under conditions of significant surface roughness of the sea. On the contrary, they are bright on a dark background in low roughness. In intermediate cases these appear as bright and dark bands.
- The wavelength between light and dark bands varies from several hundred meters to several kilometers, decreasing the magnitude from the first to the last wave.

#### 4. Study case. Internal waves in the Northern Gulf of California.

##### 4.1. Material and methods

Six SAR images from a total set of five hundred images, provided by the European Space Agency (ESA) in Fast Delivery Copy (FDC) format, with a resolution of 10m, from the ERS 2 and Envisat satellites, were selected. The selection criterion



was based on the greater stratification of the water during the warm season, which favors the formation and propagation of internal waves, so images related to the months between May and September (warm period) of 2006 were used. They were taken around 17:40 UTC in step-down, except from the 29<sup>th</sup> June to step-up at 05:30 UTC (Table I). The images are framed at the Large Islands and at the north of these, where Fu & Holt (1984) reported a greater presence.

*Table I. Information about SAR image used in the present study.*

<b>Start time UTC</b>	<b>End time UTC</b>	<b>Name</b>	<b>Date</b>	<b>Step</b>
17:38:59	17:41:01	522	22/05/2006	Down
17:39:03	17:43:07	626	26/06/2006	Down
5:26:54	5:28:28	629	29/06/2006	Up
17:41:57	17:43:50	715	15/07/2006	Down
17:39:05	17:41:06	731	31/07/2006	Down
17:41:53	17:43:45	923	23/09/2006	Down

For georeferencing and image manipulation ER Mapper software (version 7.1) was used. The georeferencing was in polynomial basis, linear order, with datum WGS84 by GEODETIC projection, with five control points. From the geo-files and the overlapping of coastline data and bathymetric data, from the National Geophysical Data Center (NGDC) of the National Oceanic and Atmospheric Administration (NOAA), we proceeded to the qualitative analysis of images through ERSI ArcMap 9.3 software. With the internal tools of this software the wavelengths between fronts, directions of propagation and the propagation velocities was measured. The directions of the propagation of the waves is determined from the curvature of the wave crests (Fu and Holt, 1984). The packet's speeds are determined assuming that the groups are formed in successive tidal cycles separated by the tidal component  $M_2$  (12.42 h). Thus, dividing the distance between groups by the tidal period, we obtain the speeds at which the front spreads (Fu and Holt, 1984; Alpers, 1985). An additional evidence to use that method, are quasi-regular spaces between the groups of wave.

The tide data, for determining the times of formation of the waves, were obtained from MAR V1.0 2011 tide prediction software in Mexico, developed by CICESE, with tide records of Bahia de Los Angeles, B.C.

#### 4.2. Study Area

The Gulf of California (GC) is a narrow sea and semi-closed, considered an evaporation basin and communicated with Pacific Ocean in the southern part (Bray, 1988). It is localized between Baja California peninsula and the Mexican states of Sonora and Sinaloa, between 23° and 32° N; 106° and 115° W. The GC is 1400 km long and its width is 100-200 km. (Figure 1). It is divided in 4 areas with significantly different characteristics. The entrance zone, in open communication with the Eastern Tropical Pacific Ocean through a line from Cabo San Lucas to Cabo Corrientes (the outer mouth), have the deeper waters (4500 m). Next to this, the Southern Gulf of California (SGC) covers from Cabo san Lucas- El Dorado line (the inner mouth) to just south of the sills of the large islands. This area consists of a series of basins with depths ranging from 2000 to 3000 m. After that, to the north, there are the Large Islands, also called Archipelago, formed principally by: Ángel de la Guarda, Tiburón, San Lorenzo and San Esteban Islands. This zone has several narrow channels, basins and sills whose maximum depths are between 300 and 900 m. Finally, the Northern Gulf of California (NGC), which has shelf sea characteristics, except in Delfín Basin, has shallow depths ranging from 300 m to few meters. Throughout the entire Gulf, the continental platform side is considerably wider than that of the peninsula.

The physiography around the Gulf, is constituted in two mountain belts parallel to the coastline, both on the mainland side where Sierra Madre Occidental is located and on the peninsula with the Sierra de Baja California. Such orography orientates the winds along the axis of the gulf, resulting in weak SE winds in summer and strong NO winds in winter (Roden, 1964). Due to this atmospheric forcing, the annual dynamic of the gulf can be divided in two seasons, warm period and cold period. Even though the important water stratification takes place during the whole year, in the warm season it is higher than in winter.

The study area of this work is framed in the Large Islands zone and in the NGC. These regions are strongly influenced by tidal dynamics. Due to the bathymetric characteristics, tidal currents cause significant mixing over the sills. Such mixing is modulated by diurnal, semidiurnal and fortnightly tidal frequencies, causing variations in the surface temperature distribution and stratification around islands (Paden *et al.*, 1991). The presence of sills among the large islands causes even stronger currents there (up to 1.5 m s<sup>-1</sup>). The strong tidal currents release large amounts of turbulent kinetic

energy, which has a tremendous impact on the physics and biology of the GC (García-Silva and Marinone, 2000).

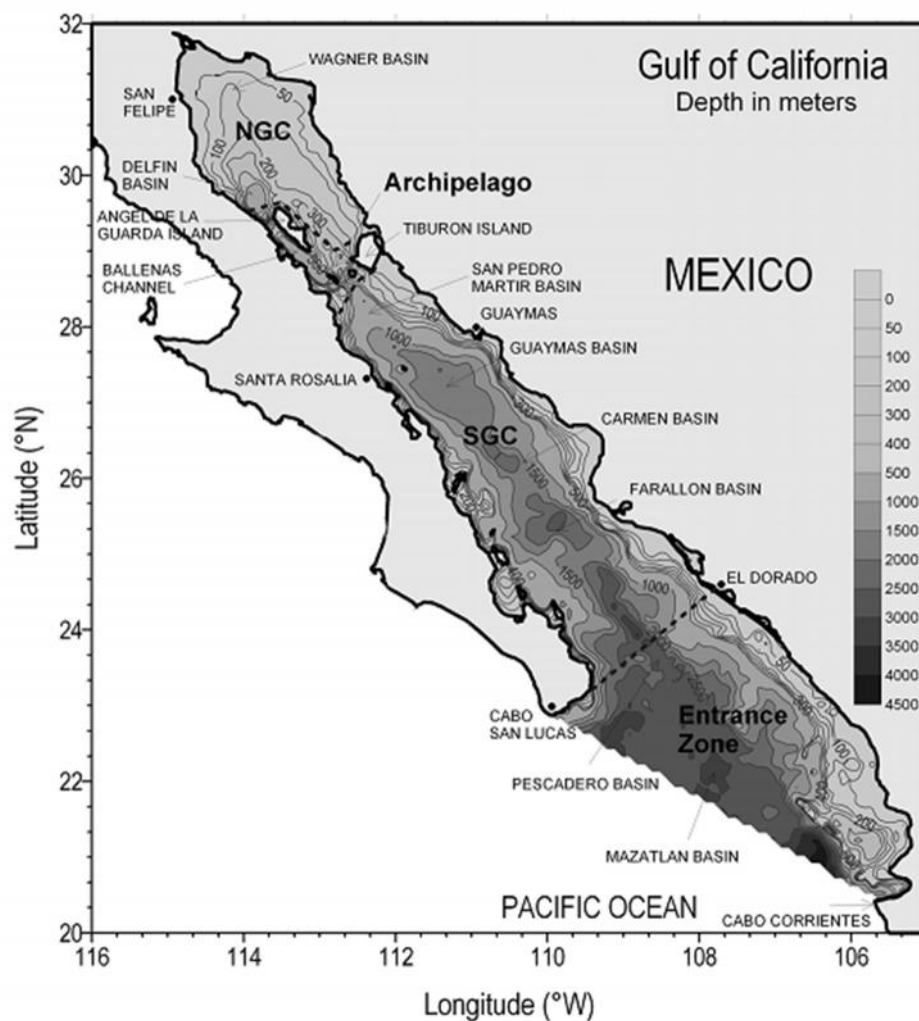
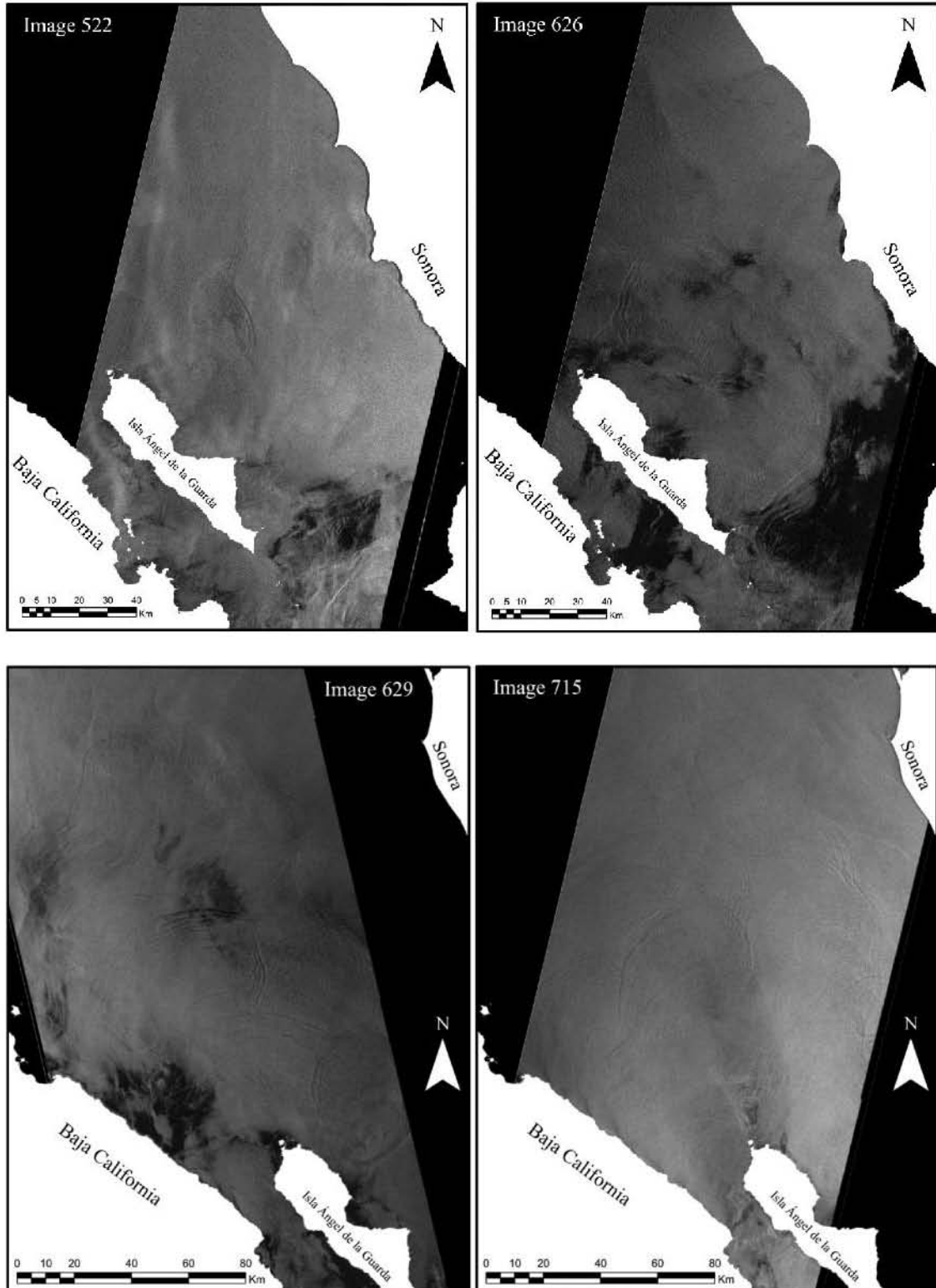


Figure 1. Bathymetry of the Gulf of California (depth in meters), its divisions and names of the basins and points of interest. Modified from Marinone and Lavin (2003).

## 5. Results

In the studied images the presence of multiple packets of internal waves has been observed (Figure 2). The wavelength of the lead waves has a range from 1 to 2.5 km, and the most common are around 1.5 km. In the particular case of image 731 have been reported wavelengths until 3 and 5 km for the second and first wave which leads the package, respectively. The wavelengths and the crests are rank-ordered, with longest at the front of the packet and shorter at its rear. The wave packets, are formed principally by 4 or 5 clearly define waves. In exceptional cases the presence of up to 14 waves in a

single packet can be seen. In addition, some images where the number of individual oscillations within the packet increases as its age increases has been observed. In other cases, the distortion in their propagation or the presence of other phenomena affecting the roughness of the water surface, such as wind, waves or atmospheric fronts make it difficult to count the exact number of oscillations.



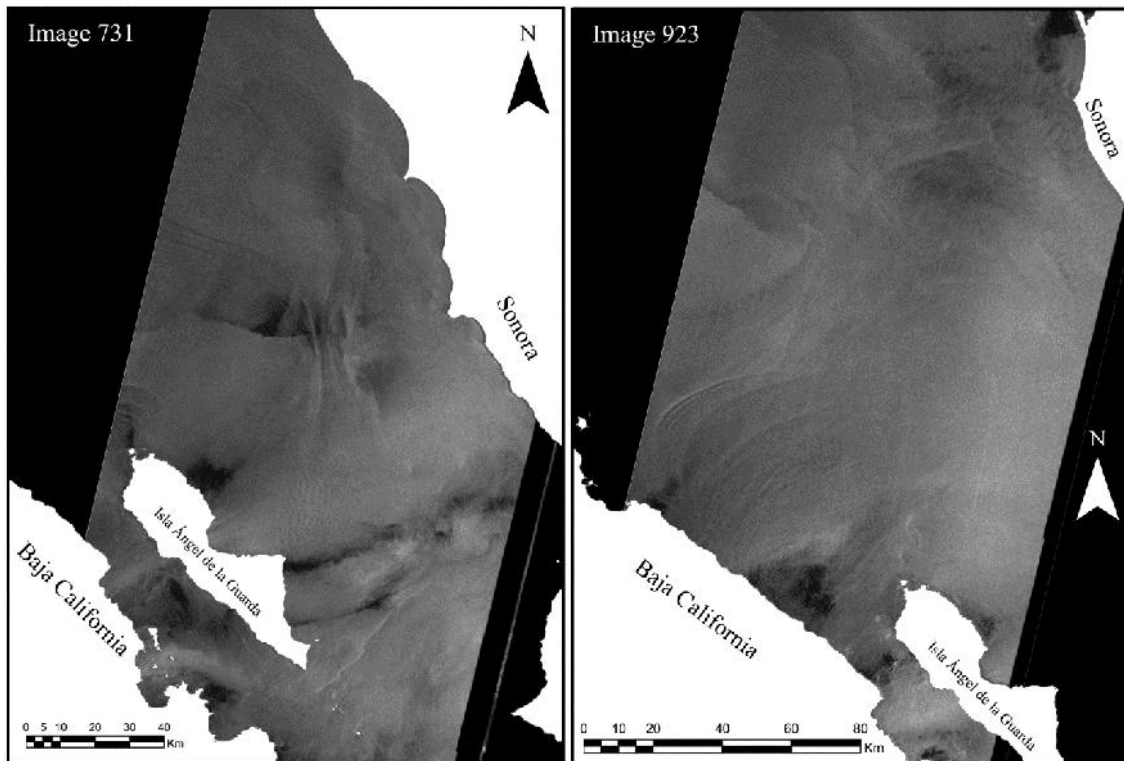


Figure 2. The Six SAR images used in the present study. Land areas in white.

Regarding spread directions, 3 main components can be defined. On the one hand, there are packages propagating to the North. These waves are present in 4 of the images, such as shown in Figure 3. In three of them (images 629, 715, 731) their formation source in the northern mouth of Ballenas channel can be clearly defined. Leaving the channel, the waves have been oriented slightly to the NE. In open sea, as they propagate northward, they can cover a range between NW and ENE.

The shape of the waves closest to the channel is not modified, while it is begun to deform when the age increases. It should be noted for the fronts that propagate northward, in the image 629, as they deformed in parallel to the bathymetric contour of 100 m. Furthermore, the distance between the fronts is reduced as these propagate to the north. Consequently the calculated velocities do too. The mean velocity of the groups is  $1.07 \text{ m s}^{-1}$ .

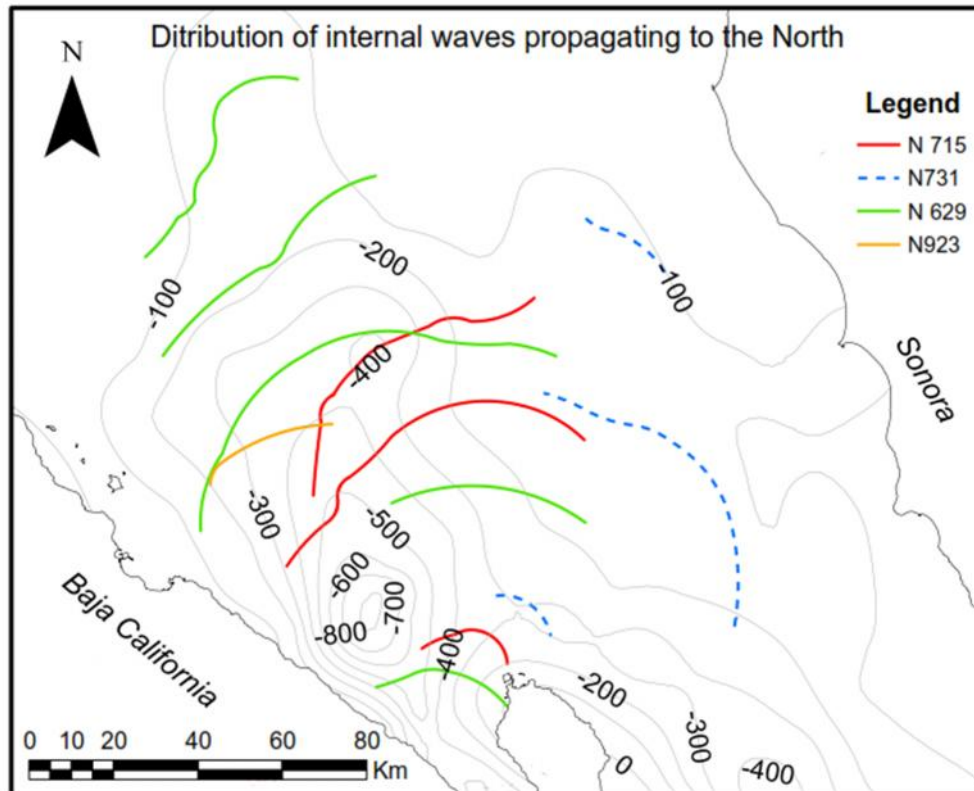


Figure 3. Fronts of the wave trains with North propagation direction. Each color corresponds to the image in which the wave appears. The dashed lines (for image 731) indicate that the SAR image didn't cover all wave, and these extends beyond the left side. ESRI ArcMap 9.3.

On the other hand, the other direction in which there have been a greater number of internal waves propagating is to the East (Figure 4). The velocities calculated for these waves are lower than the above with an average of  $0.67 \text{ m s}^{-1}$ . The spaces between fronts are also shorter and more than two packets from a same generation zone cannot be observed.

For the particular case of image 715, a positive interference between wave trains from the east and others from the northeast (in dashed lines), whose direction of propagation is unique among the studied images, can be seen. These overlapped after its formation and kept traveling together without losing its combined shape.

In the image 522, the package travelling eastward also suffers interference with other waves further south (in dashed lines). The direction of propagation of the second packages could not be established. The reason for this could be that it forms part of a semicircular wave propagating toward the SE or it could be an interference between 2 waves with independent propagation directions, E and SE.

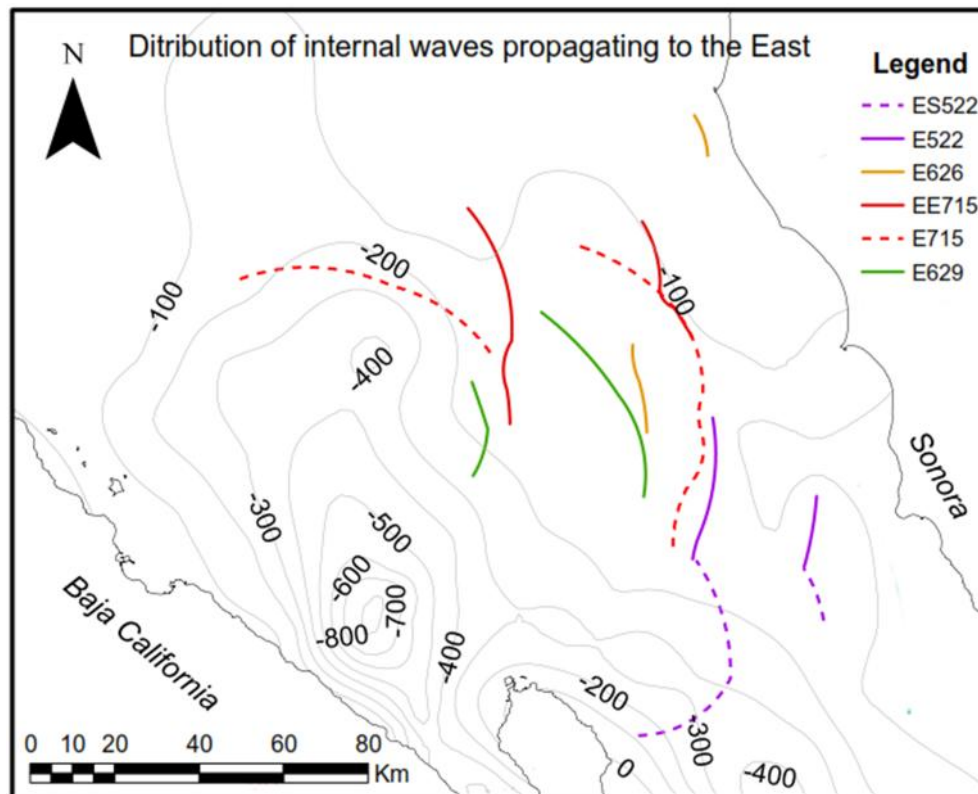


Figure 4. Fronts of the wave trains with East propagation direction. Each color corresponds to the image in which the wave appears. The dashed lines (for image 522 and 715) indicate particular features of that waves, described and discussed in the corresponding section. ESRI ArcMap 9.3.

Finally, a series of waves just north of the Ángel de la Guardia Island with propagation directions westward and northwest have been detected (Figure 5). It has not been possible to analyze the speeds of these waves because there is only a single wave package by image.

Respecting the study of tides in connection with waves, it could only be taken into account the north spread waves whose origin source is clearly defined. The first fronts of the images 629, 715 and 731 are very close to their point of formation in Ballenas channel, when the reverse flow occurs during the low tide, as shown in Figure 6.

Also, interference phenomena among waves from different sources have been observed in all the images. Such interferences have hindered the study of the spread directions and in some cases have erased the signature of the wave's presence.

Finally, solitons with an unusual configuration have been detected (image 923), whose formation frequency cannot be associate to any tidal component.

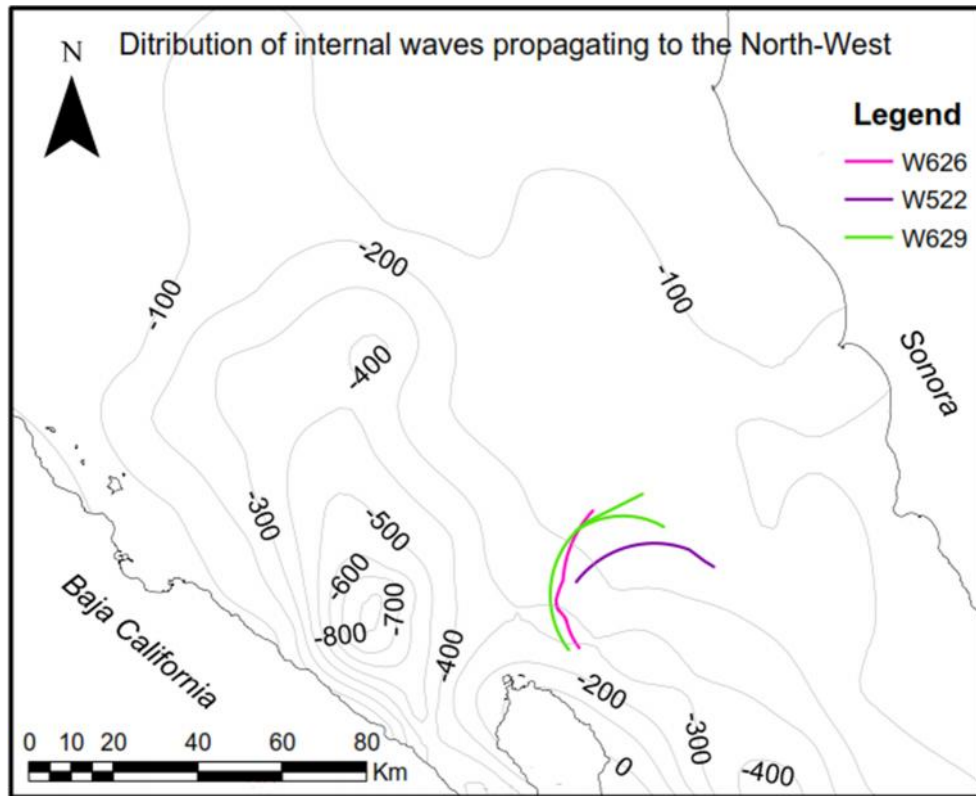


Figure 5. Fronts of the wave trains just north of the Ángel de la Guardia Island. Each color corresponds to the image in which the wave appears. ESRI ArcMap 9.3.

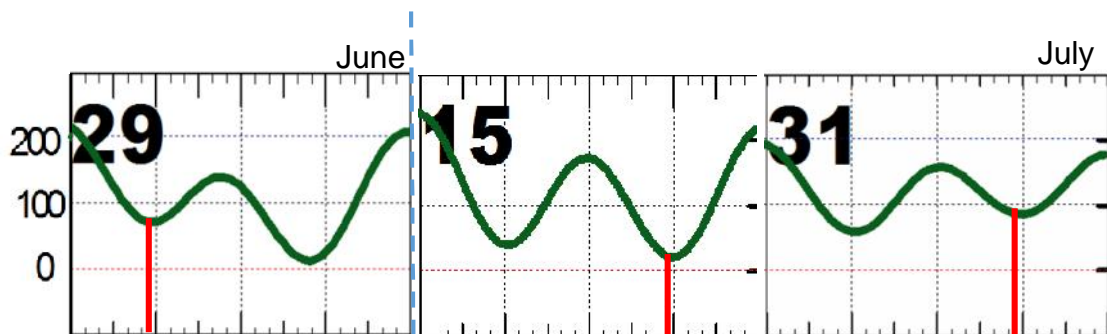


Figure 6. Tide diagrams of corresponding images days 629, 715 and 731. Time when the images were taken (red). Vertical axis in cm; horizontal axis in hours. Modified from MAR V0.9, CICESE.

## 6. Discussion

The average wavelengths coincide with the reported ones by Filonov and Lavin (2003) and Fu and Holt (1984) (1-2km). The rank-ordered and wave structure of the observed packets are according to internal wave theory. There is no explanation for the particular case of wavelengths greater than 2.5 km.



With respect to the number of oscillations per wave packet, they are much lower than those reported by Fu and Holt (1984) (10 to 20 waves), with few exceptions. Comparing the studied images with the employed by Fu and Holt, we have seen a more complex dynamic, which could be the reason why we have seen fewer oscillations per packet, because interference phenomena could mask them.

The number of individual oscillations within the packet increasing as its age increases, also coincides with internal wave theory.

The described waves propagating to the north, match with the reported by Fu and Holt (1984), whose origin is Ballenas Channel. However, although they mainly spread towards the northwest, in some images it is observed how they can spread from NW to ENE. Evidences of the Ballenas Channel as a generation point, in addition to the orientation of the wave groups, is the shape of the waves closest to the area, which is undeformed as it had no time to deform. Furthermore, the bathymetry is characterized by the presence of sills and small basins (with maximum depths of 800 m), so that such waves can be formed as Lee Waves generated when tidal flow over the sills relaxes and changes its direction. This coincides with the studied tidal records, in which the presence of these fronts emerging from the northern mouth of the channel, correspond to the moment of the reverse flow during the low tide. These results are also consistent with those of Fu and Holt (1984).

Furthermore it should be noted, that during the generation of these waves, going out from the channel, they initially diverge to the NE. This may be due to the refraction of the wave produced by the friction with Ángel de la Guarda Island shelf. At the shallowest side of the channel (at the island shelf), the east end of the wave feels the sea floor and slows while the rest of the wave continues spreading without changing its speed. This causes the wave to turn NE. Later, when the influence of the island shelf disappears, these propagate freely again. As lifetime increases, the waves begin to deform due to interference with other waves and shoaling processes. Wave shoaling effects are evidenced by the speed reduction between fronts and consequently the reduction of distance between them, as they move. On the other hand, there is evidence of wave refraction, since when the waves reach a depth of about 100-200m, the crests orientate parallel to the bathymetry, which confirms the influence of the seafloor. The average speed for these trains is very similar to that reported by Fu and Holt (1984).

Regarding trains propagating to the E, these are originated somewhere in the peninsular side. Reported velocities are significantly smaller than the packets spreading northward, and consequently also the spaces between them. This may be an early sea floor influence for a wider shelf on the continental side. This explanation agrees with the fact that no more than two packets of waves with the same origin have been seen, since they dissipate before the third packet is formed.

The interference phenomena of waves which propagate to the E, seem to follow a pattern which equally affects packages of different ages. In image 715 two fronts overlap after its formation and kept travelling together without losing its combined shape. Something similar happens in image 522, in which the same interference in the waves' structure is observed in successive fronts.

Wave packages observed just north of Ángel de la Guarda Island can relate to those described by Filonov and Lavin (2003) and Fu and Holt (1984), which spread from the basin of San Esteban. However, the described direction here, is not exactly the same. The same happens with wave's curvatures.

Finally, the solitons detected in image 923 cannot be associated to any tidal component, and their speed and wavelengths are unknown.

## 7. Conclusions

The great potential of using SAR images in the study of internal waves, to provide a synoptic picture of this phenomenon, has been proved. They enable to estimate wavelengths, speeds and number of oscillations per packet. However, its usefulness is demonstrated by the capability to study the distribution of the packets and the dominant directions of propagation.

Three main wave groups are established according to their propagation, orientation and location. These parameters have made possible to determine their formation source or at least to know the NGC region from which they propagate. Furthermore, for the first time it has been possible to relate generation moments of one group of waves with a particular tide phase.

The management of many images (about 500) has enabled to select those in which the most characteristic features of these phenomena were observed. The dynamics observed in all the images shows that it is much more complex than the one described by other authors (Filonov and Lavin, 2003; Fu and Holt, 1984). Often wave packets with different propagation directions overlap, interfering positively or negatively between them and distorting the phenomenon. This reduces its visualization or modifies the structure and orientation of the fronts, which hampers their classification according to origin and direction.

The present qualitative analysis of the distribution and characteristics of internal waves propagating north of the Large Islands, does not allow to define a definite pattern on the dynamics of this phenomenon. However, it set the basis for future studies in their description and modelling.

## 8. Acknowledgments

To the Universidad de Las Palmas de Gran Canaria for giving me the opportunity to perform this work. To the Universidad Autónoma de Baja California Sur for accepting me in their mobility program and to the Instituto Politécnico Nacional for allowing me to make this study in the Centro Interdisciplinario de Ciencias Marinas.

Concerning the development of the work, I wish to express my gratitude to the ESA (European Space Agency) for providing SAR images for the GC. Also to Diego Gámez Soto, for pretreatment of the images here employed and the unpublished observations. Also to Dr. Bernardo Germán Shirasago and Dr. Edgar Leonardo Pérez Lezama for sharing their knowledge.

## 9. Bibliography

- Alpers, W., 1985. Theory of radar imaging of internal waves. *Nature*, 314(6008), 245-247.
- Alpers, W., Wang-Chen, H., Hock, L., 1997. Observation of internal waves in the Andaman Sea by ERS SAR. In *Geoscience and Remote Sensing, 1997. IGARSS'97. Remote Sensing-A Scientific Vision for Sustainable Development.*, 1997 IEEE International (Vol. 4, pp. 1518-1520). IEEE.
- Alvarez-Borrego, S. and Schwartzlose R. S., 1979. Masas de agua del Golfo de California. *Cienc. Mar.*, 6, 43-63.

- Alvarez-Borrego, S. and Lara-Lara, J.R., 1991. The physical environment and primary productivity of the Gulf of California. In *The Gulf and Peninsular Province of the Californias*, Mem. Am. Assoc. Pet. Geol., 47, 555-567.
- Badan-Dangon, A., Dorman, C.E., Merrifield, M.A., Winant, C.D., 1991. The lower atmosphere over the Gulf of California. *Journal of Geophysical Research* 96, 16877-16896.
- Badan-Dangon, A., Koblinsky, D., Baumgartner, T., 1985. Spring and summer in the Gulf of California: observations of surface thermal patterns. *Oceanol. Acta* 8 (1), 13-22.
- Brandt, P., Alpers, W., Backhaus, J. O., 1996. Study of the generation and propagation of internal waves in the Strait of Gibraltar using a numerical model and synthetic aperture radar images of the European ERS 1 satellite. *Journal of Geophysical Research: Oceans* (1978–2012), 101(C6), 14237-14252.
- Bray, N. A., 1988. Water mass formation in the Gulf of California. *Journal of Geophysical Research: Oceans* (1978–2012), 93(C8), 9223-9240.
- Filloux, J.H., 1973 Tidal patterns and energy balance in the Gulf of California. *Nature*, 243, 217-221.
- Filonov, A. E., and Lavín, M. F., 2003. Internal tides in the Northern Gulf of California. *Journal of Geophysical Research: Oceans* (1978–2012), 108(C5).
- Fu, L. L., and Holt, B., 1984. Internal waves in the Gulf of California: Observations from a spaceborne radar. *Journal of Geophysical Research: Oceans* (1978–2012), 89(C2), 2053-2060.
- García-Silva and Marinone, S.G., 2000. Tidal dynamics and energy budget in the Gulf of California. *Cienc. Mar.*, 27, 323-353.
- Gaxiola-Castro, G., Álvarez-Borrego, S., Nájera-Martínez, S., Zirino, A. R., 2002. Internal waves effect on the Gulf of California phytoplankton. *Ciencias Marinas*, 28(3), 297-309.
- Godínez, V. M., 2011. Dinámica y termodinámica en la entrada exterior al golfo de California. Tesis Universidad autónoma de Baja California.
- Graig, P.D., 1987. Solution for internal tidal generation over coastal topography. *J. Mar. Res.*, 45(1): 83-105.
- Haury, L. R., Briscoe, M. G., Orr, M. H. (1979). Tidally generated internal wave packets in Massachusetts Bay. *Nature* 278, 312 – 317.
- Hsu, M. K., and Liu, A. K., 2004. Nonlinear internal waves in the South China Sea. National Aeronautics and Space Administration Greenbelt MD Goddard Space Flight Center.
- Jiménez Lagunes, A., 2003. Análisis de las corrientes de marea y series de temperatura en la parte norte del Golfo de California (Doctoral dissertation, M. Sc. thesis, CICESE, Ensenada, BC).
- Lavín M.F., Beier E., Badan A., 1997. Estructura hidrográfica y circulación del Golfo de California: Escalas estacional e interanual, in: Lavín, M.F. (Ed.), *Contribuciones a la Oceanografía Física de México*, Monografía UGM 3, pp.139-169.

- Lavín, M. F. and Marinone, S. G., 2003. An overview of the physical oceanography of the Gulf of California. In *Nonlinear processes in geophysical fluid dynamics* (pp. 173-204). Springer Netherlands.
- Liu, A. K., Chang, Y. S., Hsu, M. K., Liang, N. K., 1998. Evolution of nonlinear internal waves in the East and South China Seas. *Journal of Geophysical Research: Oceans* (1978–2012), 103(C4), 7995-8008.
- Lluch-Cota, S. E., 2000. Coastal upwelling in the eastern Gulf of California. *Oceanologica Acta*, 23(6), 731-740
- Marinone, S. G., 2003. A three-dimensional model of the mean and seasonal circulation of the Gulf of California. *Journal of Geophysical Research: Oceans* (1978–2012), 108(C10).
- Maxworthy, T., 1979. A note on the internal solitary waves produced by tidal flow over a three-dimensional ridge. *J. Geophys. Res.* 84, 338-346.
- Merrifield, M.A., Winant, C.D., 1989. Shelf circulation in the Gulf of California: a description of the variability. *Journal of Geophysical Research* 94, 18133-18160.
- Obeso-Nieblas, M., Shirasago-Germán, B., Gaviño-Rodríguez, J., Perez-Lezama, E., Obeso-Huerta, H., Jiménez-Illescas, Á., 2008. Variabilidad hidrográfica en Bahía de La Paz, Golfo de California, México (1995-2005). *Revista de biología marina y oceanografía*, 43(3), 559-567.
- Paden, C., Abbott, M.R., Winant, C.D., 1991. Tidal and atmospheric forcing of the upper ocean in the Gulf of California 1, sea surface temperature variability. *Journal of Geophysical Research* 96, 18337-18359.
- Pegau, W. S., Boss, E., Martínez, A., 2002. Ocean color observations of eddies during the summer in the Gulf of California. *Geophysical Research Letters*, 29(9), 6-1.
- Prasad, K. V. S. R., and Rajasekhar, M., 2006. Observations of Oceanic Internal Waves in Bay of Bengal using Synthetic Aperture Radar. In *Advances in SAR Oceanography from Envisat and ERS Missions* (Vol. 613, p. 13).
- Ramírez-Manguilar, A. M., 2000. Análisis armónico de datos de corrientes en la región norte del Golfo de California de noviembre de 1994 a febrero de 1996 (Doctoral dissertation, B. Sc. thesis, 56 pp., Fac. de Cienc. Mar., Univ. Autónoma de Baja Calif., Ensenada, Mexico).
- Roden G.I., 1964. Oceanographic aspects of the Gulf of California, in: Van Andel T.H., Shor G.G. (Eds.), *Marine Geology of the Gulf of California*, Mem. Am. Ass. Petrol. Geol. 3, pp. 30-58.
- Sandstrom, H., and Elliott, J. A., 1984. Internal tide and solitons on the Scotian Shelf: A nutrient pump at work. *Journal of Geophysical Research: Oceans* (1978–2012), 89(C4), 6415-6426.
- Shirasago, B., 1996. Aplicaciones del radar de apertura sintética (SAR) del satélite ERS-1 al estudio de la dinámica superficial de mesoescala en el Mediterráneo occidental. *Publicacions de la Universitat de Barcelona*.
- Steinberg, B. D., 1976. Principles of aperture and array system design: Including random and adaptive arrays. New York, Wiley-Interscience, 1976. 374 p., 1.

Trask, R. P., and Briscoe, M. G., 1983. Detection of Massachusetts Bay internal waves by the synthetic aperture radar (SAR) on SEASAT. *Journal of Geophysical Research: Oceans* (1978–2012), 88(C3), 1789-1799.

Turrent-Thomson, C., 1996. Análisis estadístico de observaciones de corrientes y temperatura en la parte norte del Golfo de California (Doctoral dissertation, B. Sc. thesis, 67 pp., Fac. de Cienc. Mar., Univ. Autónoma de Baja Calif., Ensenada, Baja California, Mexico).

Zamudio, L., Hogan, P., Metzger, E. J., 2008. Summer generation of the Southern Gulf of California eddy train. *Journal of Geophysical Research: Oceans* (1978–2012), 113(C6).

# Memoria final del Trabajo Fin de Grado (TFG)

---

GRADO EN CIENCIAS DEL MAR. ASIGNATURA: 40630 - Trabajo Fin de Grado

Año Académico: 2013/2014 Alumno: Pol Carbó Mestre

## 1. Descripción detallada de las actividades desarrolladas durante la realización del TFG

Las prácticas se realizaron en el departamento de Oceanología, laboratorio de oceanografía física a cargo del Dr. Bernardo Shirasago Germán, tutor de prácticas, en el Instituto Politécnico Nacional, Centro Interdisciplinario de Ciencias Marinas.

Las actividades desarrolladas durante la estancia de prácticas, teniendo en cuenta, en su caso, el secreto profesional al que está obligado, son las siguientes:

### *a) Introducción a la percepción remota espacial.*

Con el objetivo de conocer el estudio de los océanos a través de herramientas satelitales y posteriormente aplicarlo a los estudios desarrollados en mi laboratorio así como sus aplicaciones al TFG, se procedió a la lectura de trabajos en estos campos, centrándose principalmente en Synthetic Aperture Radar (SAR). Para ello, se me aseguro el acceso a los recursos digitales y físicos del centro, así como a las suscripciones de revistas científicas. Para completar la formación se asistió a la asignatura de percepción remota que el CICIMAR ofrece para las titulaciones de Master que aquí se cursan

### *b) Análisis de la dinámica de mesoescala del Golfo de California.*

El área de estudio se ubica en el Golfo de California (GC). Por ello, con el objetivo de comprender la dinámica del Golfo de California, parte fundamental del TFG que se incluye para comprender la presencia de ondas internas en el golfo, se dedicó una serie de horas establecidas en el cronograma de las prácticas a la lectura de trabajos en el campo de la oceanografía física del GC. Centrándose principalmente en los procesos de afloramiento, generación de remolinos, dinámica mareal, estacionalidad de los fenómenos y ondas internas. Para ello, se me aseguro el acceso a los recursos digitales y físicos del centro, así como a las suscripciones de revistas científicas. Además se dedicaron horas extras para la

asistencia del curso en oceanografía física que oferta CICIMAR para las titulaciones de Master. También se asistió a los seminarios que cada semana se realizan en el centro.

c) *Estudio de las ondas internas.*

La falta previa de conocimientos acerca de este fenómeno, hizo necesario dedicar una serie de horas al estudio de las ondas internas centrándose principalmente en ondas internas oceánicas, para poder alcanzar los objetivos del TFG. Independientemente de las regiones de formación, el estudio se centró, en características de las ondas, condiciones para su formación, puntos de formación, propagación y disipación, además de los sistemas de detección y cuantificación. Para ello, se me aseguro el acceso a los recursos digitales y físicos del centro, así como a las suscripciones de revistas científicas.

d) *Introducción al manejo de los Sistemas de Procesamiento de Imágenes de Satélite ERMapper, junto a ArcMap y MarV10, programas necesarios para el desarrollo de tareas del TFG.*

Para poder llevar a cabo las tareas relacionadas con el manejo de las imágenes de SAR se tuvo que aprender a manejar el software ER Mapper. Con estas se trató y georeferenció las 6 imágenes empleadas para el estudio. Al mismo tiempo, para poder relacionar la información extraída de tales imágenes, con las características batimétricas de la región y su relación con las mareas se emplearon respectivamente los programas ESRI ArcMap 9.3 y MarV10, los cuales también se partió de cero en el aprendizaje de su manejo. Para ello se dispuso de un centro propio de trabajo equipado por el departamento con un ordenador de sobremesa y un monitor de televisión de alta resolución. Además de las licencias de instalación en mi ordenador personal.

e) *Capacitación en el conocimiento y uso de datos de sensores activos, básicamente Radar de Apertura Sintética.*

Con el fin de extraer resultados de las imágenes de SAR empleadas para el trabajo, fue necesario aprender el funcionamiento de los sistemas SAR, como estos pueden detectar ondas internas y aprender a reconocerlas en las imágenes. A través de



los recursos bibliográficos y la asistencia del tutor de empresa y otro personal del centro, pude alcanzar estos objetivos.

## 2. Formación recibida (cursos, programas informáticos, etc.)

*Cursos:* Asistencia a los cursos del Master en Ciencias en Manejo de Recursos Marinos.

- 1753. Oceanografía Física. Coordinador de la asignatura: Dr. Bernardo Shirasago Germán. Profesores: Dr. Bernardo Shirasago Germán, Dr. Maclovio Obeso Nieblas y Dr. Ángel Rafael Jiménez Illescas.
- 10A6075. Oceanografía Satelital. Coordinador de la asignatura y profesor: Dr. Bernardo Shirasago Germán.

*Programas informáticos:*

- ER Mapper 7.1. ER Mapper es una aplicación de procesamiento de imágenes de gran alcance, para la extracción de información cuantitativa ajustada a un campo geoespacial. Este software permite visualizar y mejorar los datos de mapa de bits, visualizarlos, editar datos vectoriales y enlazarlos con datos geoespaciales, además incluye un sistema de gestión de bases de datos. Esta herramienta se empleó para el tratamiento y estudio de las imágenes de SAR en formato FDC (Fast Delivery Copy).
- MarV10. El software MAR V1.0 2011 de predicción de Mareas en México, desarrollado por el CICESE, se empleó para la obtención de datos de marea y la determinación de los momentos de formación de las ondas internas en la región estudiada para el TFG.
- ESRI ArcMap 9.3. Este constituye el principal componente de ArcGIS, conjunto de programas de procesamiento geoespacial, usado principalmente para la visualización, edición, creación y análisis de datos geoespaciales. Se empleó para la conjugación de datos batimétricos y de línea de costa sobre las imágenes de SAR previamente tratadas en ER Mapper, además de la edición de dichas imágenes y vectorización de alguno de sus componentes.

### 3. Nivel de integración e implicación dentro del departamento y relaciones con el personal.

Las relaciones con los compañeros de trabajo y personal asociado al departamento, así como con el tutor de prácticas siempre fueron desde un trato cordial y amable desde el primer momento, lo que permitió una rápida integración en el centro y en el equipo de trabajo. La implicación en el departamento queda patente en la asistencia a los seminarios de los profesionales y alumnos del mismo, en la colaboración mutua ante dudas y problemas relacionados con los trabajos. En ningún momento se ha tenido ningún problema relacionado con el personal del centro por motivos de conducta o trato.

Además la implicación con los proyectos desarrollados aquí, estrechamente relacionados con el TFG, ha supuesto la participación en la modalidad poster en el XVIII Congreso Nacional de Oceanografía que se llevara a cabo en La Paz, del 4 al 6 de junio de 2014. El título del trabajo presentado en este congreso, cuyos resultados son los obtenidos para el TFG, es: Detección de ondas internas con radar de apertura sintética (SAR) en el norte del golfo de california y las grandes islas.

También existe bastante interés en realizar una publicación conjunta con mi tutor de empresa y otros compañeros de laboratorio, empleando parte de los resultados que se obtuvieron para el TFG, en la revista *Current Developments in Oceanography*. No obstante aún se está evaluando el plan de actuación.

### 4. Aspectos positivos y negativos más significativos relacionados con el desarrollo del TFG.

Los aspectos positivos más significativos relacionados con el desarrollo de las prácticas, han sido el clima de trabajo en el laboratorio. Esto es así debido a la disponibilidad del personal y del tutor a la hora de resolver cualquier duda o solventar un problema y al ofrecer todos los recursos que estén en sus manos. También la libertad horaria que me han ofrecido, siempre que se cumpliera la dedicación total establecida.

Por otro lado, la disponibilidad de recursos y herramientas para trabajar ha favorecido positivamente el desarrollo de las prácticas.

Otros aspectos positivos han sido el aprendizaje de un nuevo campo en el estudio oceanográfico, como es la percepción remota, y que desgraciadamente ya no se oferta en el plan de estudios del Grado en Ciencias del Mar de la ULPGC. Además, de afianzar conocimientos ya adquiridos a lo largo de la carrera.

## 5. Valoración personal del aprendizaje conseguido a lo largo del TFT.

Los conocimientos adquiridos a lo largo de la estancia han permitido ampliar mis perspectivas de futuro, al conocer mejor la diversidad de campos de estudio dentro de la oceanografía física, en los que uno se puede especializar. También me han permitido profundizar en el campo de la oceanografía física y especializarme en sensores remotos, principalmente en imágenes de Radar. Al mismo tiempo, el aprendizaje en el manejo de nuevos software siempre es útil, aun cuando no vuelva a tener oportunidad de emplearlos, ya que mejora la agilidad en el uso y entendimiento del funcionamiento de este tipo de programas. Concretamente para el caso del software ESRI ArcMap 9.3, el aprendizaje de su manejo ha sido una ampliación de los contenidos que oferta la asignatura Técnicas de Información Geográfica en el Ámbito Geológico, permitiendo terminar la carrera sabiendo emplear los dos principales soportes virtuales para el desarrollo proyectos de Sistemas de Información Geográfica (SIG). Otro aspecto de la formación a valorar es la adaptación y el aprendizaje de la dinámica de trabajo en una institución científica y en proyectos de carácter científico.

Además el hecho de haber realizado las prácticas en un centro interdisciplinario me ha permitido aprender de otras ramas de las ciencias marinas hasta el punto de replantearme mi futura especialización tras terminar la carrera. Concretamente los campos de la ecología o la oceanografía biológica estaban estrechamente relacionados con los proyectos de teledetección que se trabajaban en mi laboratorio.